Real-time optimal charging strategy for a fleet of electric vehicles minimizing battery degradation

Subhajeet Rath †, Róbinson Medina †, Steven Wilkins †,‡

† Powertrains Department, TNO

‡ Electrical Engineering department, Eindhoven University of Technology
Emails: † {Subhajeet.Rath, Robinson.Medina, Steven.Wilkins}@tno.nl

Abstract—The electrification of the transportation industry has emerged as a promising solution to reduce automotive emissions. However, this transition presents various challenges, such as the limited availability of charging infrastructure, grid capacity, and the high total cost of ownership for Battery Electric Vehicles (BEVs), primarily due to the cost of the battery. This study proposes an algorithm that generates charging schedules for a fleet of BEVs during their operational period to address these challenges. The algorithm provides a time frame and charging power for all vehicles in the fleet, which can optimize the use of charging infrastructure, distribute the grid load throughout the day, and reduce BEV operational costs by extending the battery lifetime. The algorithm was tested in a realistic case study within the European project URBANIZED. Simulation results shows a saving of 13% on the total cost of charging. Furthermore, the algorithm's execution time was less than 160 seconds for a fleet of 200 vehicles, considered real-time for a fleet charging operation. In conclusion, this algorithm offers a viable solution to address challenges in the electrification of the transportation industry. Fleet managers can benefit from its costsaving benefits and efficient execution time, making it a promising tool for transitioning to BEVs.

Index Terms—Battery electric vehicles, Optimized charging scheme, Real-time, Battery degradation, Grid congestion

I. INTRODUCTION

Greenhouse Gas Emission (GGE) are known to cause significant negative impact on the environment and are one of the major contributors to climate change [1]. These emissions are generated by different sectors of the economy, including transportation, agriculture, and energy generation. Of these sectors, the transportation sector is a major contributor to GGE due to the prevalent usage of Internal Combustion Engine (ICE) in most modern vehicles [2]. In recent years, Battery Electric Vehicle (BEV) have been identified as a potential mitigation technology for this problem, as they have lower well-to-wheel GGE emissions than ICE vehicles [3]. However, the complete adoption of BEVs still faces several challenges, including the high initial costs associated with battery prices and limitations on grid capacity, as seen in the Dutch case [4], [5]. These challenges are particularly relevant in commercial applications, such as delivery companies and bus operators, which require large fleets of BEVs. This paper specifically focuses on the challenges and opportunities associated with BEV fleet adoption.

979-8-3503-1997-2/23/\$31.00 ©2023 IEEE

To overcome the limitations on grid capacity and battery costs, one effective strategy is to control the charging dynamics of BEV fleet via charging schedules. Such schedules must ensure that: i) the power required for charging the fleet is distributed according to the grid capacity throughout the day [6]; ii) individual vehicle timings (i.e., different arrival and departure times) are taken into account, ensuring compliance with fleet operation requirements; iii) the algorithm used to compute the schedule can execute in real-time, making it useful for the fleet operator; and iv) battery degradation is minimized. For delivery companies, item ii) and iii) become even more relevant, as vehicle timings vary on a daily basis. Battery degradation is a critical concern for any commercial application, as it directly affects the total cost of fleet ownership. This degradation is triggered by two factors: high crate (charge/discharge power during battery operation), leading to cyclic ageing, and high State-of-Charge (SoC) over an extended period of time, leading to accelerated calendar ageing [7].

Designing charging strategies has been previously studied in literature such as [8], [9]. [8] focused on optimal charging considering grid-capacity limitations, using a distributed optimization problem. [9] describes an algorithm to determine the size, routing and operation of an electric bus fleet. Both approaches do not consider battery degradation in their strategies. Only few research work have considered battery ageing in the charging schedule problem. [10] presents an age-aware optimization algorithm for buses, which was later extended in [11]. The algorithm includes variable departure and arrival time as well as considerations for execution time of the algorithm. However, in both approaches, cyclic ageing is not considered because the charging rate is limited to very low c-rates, which is generally not applicable. [12] presents an optimal electric-bus fleet scheduling strategy that considers battery degradation and non-linear charging time. Like in the previous case, the effects due to cyclic ageing are not considered and the charging rate seems to always be the nominal charger power. [13] presents an optimal charging strategy for a BEV fleet which considered battery degradation (calendar and cyclic ageing) and grid constraints. However, the battery ageing model used, as well as the cost-function are highly non-linear, which makes solving the optimization problem computationally too expensive and potentially unfeasible for large fleets. Moreover, the optimization algorithm requires that all the vehicles are connected and disconnected at the same time. None of the approaches described above, considers all effects on battery ageing, real-time execution time and individual timing requirements per vehicle.

This paper presents an optimal charging schedule algorithm for BEV fleets that minimizes battery degradation (calendar and cyclic ageing), guarantees individual timings (i.e., departure and arrival times) per vehicle, and satisfies grid limitations. The optimization algorithm shows the following novelties:

- An optimization strategy that is separated into linear and non-linear integer problem. The linear part generates a charging profile which minimizes cost due to cyclic ageing. The non-linear integer part finds a valid time slot to comply with grid capacity restrictions and minimizes cost due to calendar ageing.
- An ageing model that is simplified to only account for effects from the charging process.

The resulting algorithm has an execution time that can be considered real-time, for the time scale of the scheduling problem.

The rest of the paper is divided as follows: Section II presents the models used by the optimization algorithm. The optimization problem and the solution methodology is described in Section III, as well as the battery-ageing model simplification. Section IV introduces a realistic case study as well as simulation results. The paper closes with conclusions in Section V.

II. SYSTEM MODELLING

In this section, several mathematical models describing the electrical, thermal and ageing behaviour of a battery pack are discussed. Additionally, a simplified model for a charger is also developed. These models are used to compute the total cost of charging in Section III.

A. Electrical Model

The battery pack in a BEV consists of individual cells configured in series and parallel. Each cell is modelled as a two RC Equivalent Circuit Model (ECM) as shown in Fig. 1. The dynamics of the system can be described as

$$U_{cell} = U_{oc} + I \cdot R_0 + U_1 + U_2, \tag{1}$$

where U_k $(k \in \{1, 2\})$ is calculated as

$$\dot{U_k} = \frac{I}{C_k} + \frac{U_k}{R_k \cdot C_k} \tag{2}$$

Here, U_{cell} and I are the terminal voltage and current of the cell, respectively, U_k , R_k and C_k are the voltage, resistance and capacitance across R_kC_k circuit, respectively. R_0 is the Ohmic resistance and U_{ocv} is the open circuit voltage. All units are assumed in the international system, unless otherwise stated.

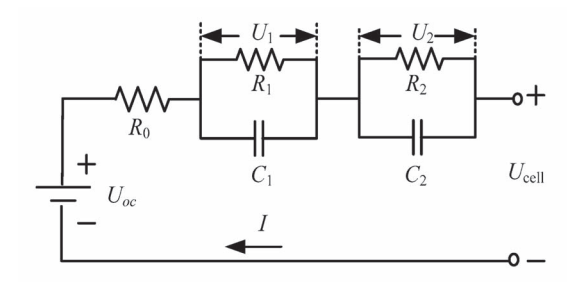


Fig. 1: Schematic of a 2 RC ECM [14].

B. Thermal Model

The battery pack is represented with a lumped-mass thermal model as shown in Fig. 2. The dynamics of this system is formulated as

$$C_P \dot{T_P} = \frac{T_a - T_P}{R_{Pa}} + \dot{Q}. \tag{3}$$

Here T_P and T_a are the temperature of battery pack and ambient respectively, C_P is the thermal heat capacity of the pack, R_{Pa} is the thermal resistance between the pack and ambient and \dot{Q} is the total internal heat generated by the battery pack, further defined by

$$\dot{Q} = (\dot{Q_P} + \dot{Q_S}) \cdot N_{cell},\tag{4}$$

where N_{cell} is the number of cells, $\dot{Q_P}$ and $\dot{Q_S}$ are the internal heat generated by overpotential and change in entropy, respectively [15]. The heat generation due to overpotential is expressed as

$$\dot{Q}_P = (U_{cell} - U_{oc}) \cdot I, \tag{5}$$

while the entropic heat generation is given as

$$\dot{Q_S} = I \cdot T_P \cdot \frac{dU_{oc}}{dT_P}.$$
(6)

Here, U_{cell} and U_{oc} are the terminal and open circuit voltage of a cell respectively, I is the terminal current and dU_{oc}/dT_P is the entropic heat coefficient.

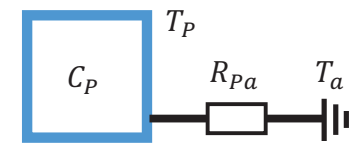


Fig. 2: Schematic of a lumped-mass thermal model for a battery pack.

C. Ageing Model

Over the course of its lifetime, the performance of a battery deteriorates due to irreversible changes to its electro-chemistry. This phenomenon is called battery ageing. There are two types of ageing processes: calendar and cyclic ageing. Calendar ageing occurs during the lifetime of the battery due to unintended side reactions that consumes its lithium. Cyclic ageing occurs during the operations of the battery (charging and discharging)

due to anode layer formation which reduces its total capacity. Both phenomenon reduces the charge capacity which is an indication of battery heath. The normalized battery charge capacity is defined as

$$\tilde{C}_B = C_B/\bar{C}_B,$$

where \bar{C}_B is the capacity of a new battery in kWh and C_B is the current capacity of the battery. Any ageing mechanism results in a drop in capacity denoted by $\Delta \tilde{C}_B$. According to [16], this drop in capacity due to calendar ageing is

$$\Delta \tilde{C}_B = \alpha_{cap} \cdot t^{0.75},\tag{7}$$

and cyclic ageing is

$$\Delta \tilde{C}_B = \beta_{cap} \cdot \sqrt{Q}. \tag{8}$$

Here, Q is the charge throughput in Ah and t the elapsed time during the ageing event. α_{cap} and β_{cap} are defined as

$$\alpha_{cap} = (a_1 \cdot z - a_2) \cdot 10^{-6} \cdot e^{-a_3/T_P}$$

$$\beta_{cap} = b_1 \cdot (\varnothing z - b_2)^2 + b_3 \cdot \Delta z$$

$$+ b_4 \cdot Crate_{ch} + b_5 \cdot Crate_{dch} + b_6.$$
(10)

Here, z and T_P are SoC and battery pack temperature contributing to calendar ageing. $\varnothing z$ is the average SoC, Δz is the Depth of Discharge (DoD), and $Crate_{ch}$ and $Crate_{dch}$ are the c-rate during a full charge and discharge cycle, respectively. a_x and b_y are several battery-specific ageing parameters.

D. Charger Model

A charger model describes the relationship between input and output power for a charger expressed as an efficiency map. An example of such a map in a normalized form is shown in Fig. 3. In this work, the efficiency map is scaled to represent a charger of 11 kW. Fig. 4 shows a plot between input to output power of the charger. It is seen that a linear fit can approximate this data as

$$P_G = m_c \cdot P_c + b_c, \tag{11}$$

where P_G is the power drawn from the grid, P_c is the charge power output to the BEV and m_c and b_c are fitting constants.

III. OPTIMIZATION PROBLEM

The objective of the optimization problem is to find a charging schedule which minimizes the cost for operations while charging the fleet of BEVs. Before the optimization problem is defined, some general requirements are introduced.

A. Problem requirements

Fig. 5 shows an example of a scheduling requirement for a fleet of BEVs. Let $\mathbb{V}=\{1,2,\ldots,N\}$ be a set of N vehicles, which can arrive into a charging hub at a certain start time and leave at an end time. This provides a charging window within which the vehicles must be charged. Each vehicle $i\in\mathbb{V}$ has an initial SoC (\underline{z}^i) at the time of entering and a target SoC (\overline{z}^i) which should be reached before they leave the charging hub. It is assumed that the number of chargers are equal to the vehicles.

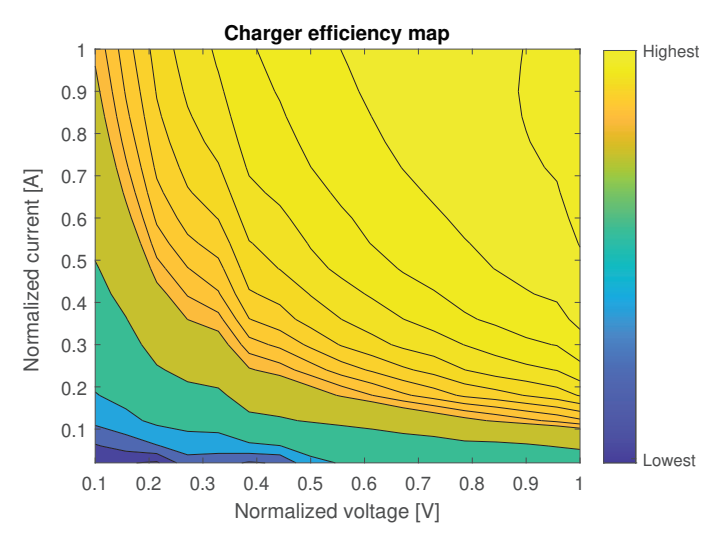


Fig. 3: Example of a normalized efficiency map of a charger.

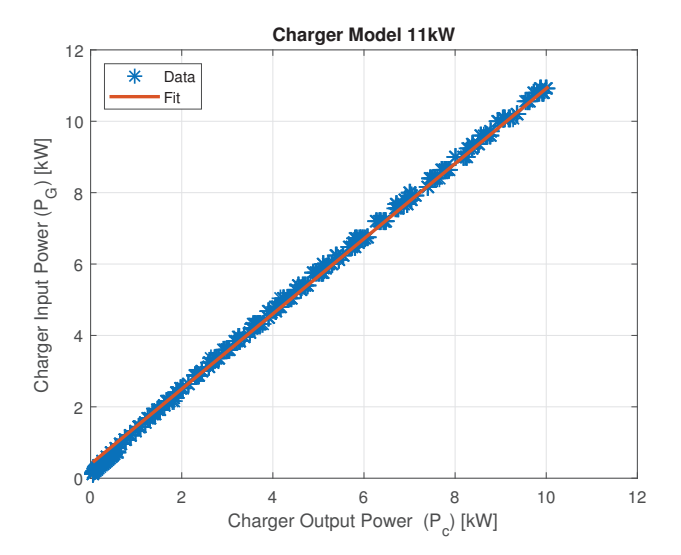


Fig. 4: Charger model as a linear fit between input and output efficiency.

The time duration for charging the vehicle has been divided into discrete segments of equal length (e.g., $15 \, \mathrm{min}$). Let \mathbb{T} be a set of all time segments in which a vehicle can be charged. The vehicle $i \in \mathbb{V}$ can be charged in a subset of \mathbb{T} . This set can be described as $\mathbb{T}_i \subseteq \mathbb{T}$ and has n^i elements. The control variable for the optimization problem is the vector $\mathbf{P_c}$, which contains the charge power for all the time segments for each vehicle, i.e.,

$$\mathbf{P_c} = \begin{bmatrix} i \\ j P_c \end{bmatrix}, i \in \mathbb{V} \land j \in \mathbb{T}_i.$$
 (12)

B. Problem Definition

In this work, the objective of the optimization problem is to minimize two types of cost: cost due to electricity from the grid and cost due to battery degradation.

The cost of electricity to charge the vehicle is

$$\mathcal{J}_{el} = \mathcal{E}_{el} \cdot P_G, \tag{13}$$

Time	09	:00 09	:15 09	:30 •		20	:00 2	0:15 20	:30
Vehicle 1			\underline{z}^1				\overline{z}^1		
Vehicle 2	\underline{z}^2					\overline{z}^2			
Vehicle <i>i</i>		\underline{z}^i			$_{j}^{i}P_{c}$			\overline{z}^i	
Vehicle N				\underline{z}^N					\overline{Z}^N

Fig. 5: BEV fleet charging requirements. The time segments available for charging are shown in green.

where \mathcal{E}_{el} is the time-varying price of electricity and P_G is the power drawn from the grid. Fig. 6 shows an example of the variation of electricity price during a day. In this case, it can be seen that the night time costs are lower then day time costs. Applying the charger model of (11) to (13), the cost of electricity is expressed as

$$\mathcal{J}_{el} = \mathcal{E}_{el} \cdot (m_c \cdot P_c + b_c). \tag{14}$$

From optimization theory, the minimum of (14) is independent of the constant term b_c . Hence, the cost function is reformulated as

$$\mathcal{J}_{el} = \mathcal{E}_{el} \cdot m_c \cdot P_c. \tag{15}$$

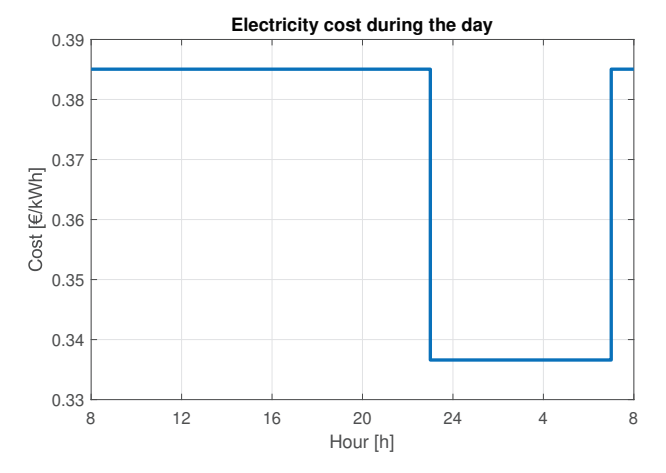


Fig. 6: Example of electricity price during a day.

The costs associated with battery degradation is defined in terms of the loss of investment for a fleet operator. As degradation of a battery brings a reduction in its usability, the fleet operator eventually losses the investment cost on the battery. The cost due to battery degradation is expressed as

$$\mathcal{J}_{deg} = \mathcal{E}_{bat} \cdot \Delta \tilde{C}_B / \tilde{C}_B^{eff}, \tag{16}$$

where \mathcal{E}_{bat} is the effective battery cost and is defined as $\mathcal{E}_{bat} = \mathcal{E}_{bat}^{buy} - \mathcal{E}_{bat}^{sell}$. \mathcal{E}_{bat}^{buy} is the cost at which the battery was bought and \mathcal{E}_{bat}^{sell} is the cost at which the battery can be sold at the end of its life. \tilde{C}_B^{eff} is the required capacity drop (normalized) after which the battery is considered at its End-of-Life (EoL). For automotive application 80 % capacity $(\tilde{C}_B = 0.8)$ is considered EoL. Hence, \tilde{C}_B^{eff} for an automotive

battery is 0.2. In Section II-C, two types of degradation mechanisms are established: calendar and cyclic ageing. Both of them have the same cost function (16) with different $\Delta \tilde{C}_B$. Replacing $\Delta \tilde{C}_B$ from (7 and 8) into the cost function (16), the degradation cost for calendar and cyclic ageing are

$$\mathcal{J}_{ca} = \mathcal{E}_{bat} \cdot \alpha_{cap} \cdot t^{0.75} / \tilde{C}_B^{eff}, \tag{17}$$

$$\mathcal{J}_{cy} = \mathcal{E}_{bat} \cdot \beta_{cap} \cdot \sqrt{Q} / \tilde{C}_{B}^{eff}, \tag{18}$$

where, \mathcal{J}_{ca} is the cost for calender ageing while \mathcal{J}_{cy} is the cost for cyclic ageing.

Fig. 7 shows a generic drive cycle for battery operation. The ageing model described in Section II-C calculates the deterioration for such a full drive cycle. However, the fleet scheduling algorithm only impacts the charging part of the drive cycle with the objective to regain the lost SoC during the discharge part. Hence, a charge cycle generated by fleet scheduling algorithm cannot influence $\varnothing z$, Δz and $Crate_{dch}$. Additionally, $Crate_{ch}$ can be approximated as

$$Crate_{ch} = Pc/\bar{C}_B$$
.

These assumptions are applied to the ageing model (9 and 10) and substituted into cost function (17 and 18) which is expressed as

$$\mathcal{J}_{ca} = \mathcal{E}_{bat} \cdot a_1 \cdot z \cdot 10^6 \cdot e^{-a_3/T_P} \cdot t^{0.75} / \tilde{C}_B^{eff}, \tag{19}$$

$$\mathcal{J}_{cy} = \mathcal{E}_{bat} \cdot b_4 \cdot (Pc/\bar{C}_B) \cdot \sqrt{Q}/\tilde{C}_B^{eff}. \tag{20}$$

During the charging process, the charger limits minimum and maximum output power (\underline{P}_c and \bar{P}_c). However, if the vehicle is not charging the charge power is set to zero. This range of charge power can be defined as a set $\mathbb{P}_c = \{0\} \cup \{[\underline{P}_c, \bar{P}_c]\}$. All elements of vector \mathbf{P}_c should be within this set which is defined as constrain

$$\mathbf{P_c} \in \{\mathbb{P}_c\}^n \tag{21}$$

where n is the number of elements in vector $\mathbf{P_c}$ and can be computed as

$$n = \sum_{i=1}^{N} n^{i}$$

.

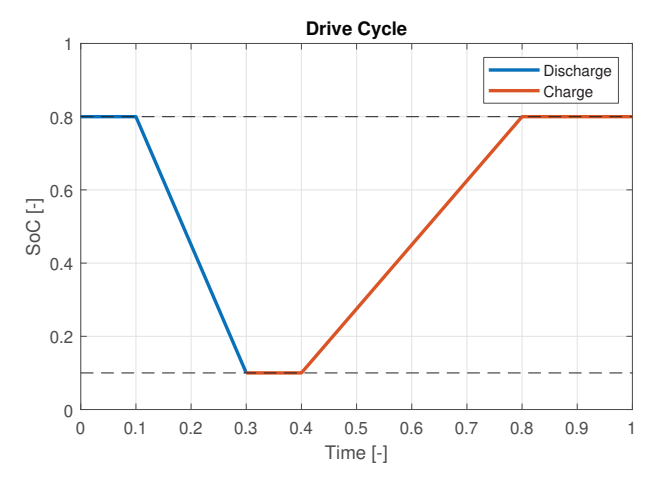


Fig. 7: Generic drive cycle for a battery operation.

There is also a limit on the maximum power that can be cumulatively drawn from the grid. At a given time segment this constraint is expressed as

$$\sum_{i=1}^{N} {}_{j}^{i} P_{G} \le \bar{P}_{G}, \ \forall \ j \in \mathbb{T}$$
 (22)

where \bar{P}_G is the maximum grid capacity. Replacing (22) with (11), the constraint becomes

$$\sum_{i=1}^{N} {}_{j}^{i} P_{c} \le \hat{P}_{G}, \ \forall \ j \in \mathbb{T}$$
 (23)

where $\hat{P}_G = (\bar{P}_G - b_c)/m_c$. It should be noted that from (12), the variable ${}^i_j P_c$ does not exist for all $j \in \mathbb{T}$. The constrain (23) is only evaluated for a vehicle $i \in \mathbb{V}$ when $j \in \mathbb{T}_i$ is also true.

The charging process must result in the vehicle SoC z^i reaching at least \bar{z}^i without exceed 1. Here, z^i is calculated as

$$z^{i} = \underline{z}^{i} + \sum_{j \in \mathbb{T}_{i}} {}_{j}^{i} P_{c} / \bar{C}_{E} \cdot \Delta t_{c}, \ \forall \ i \in \mathbb{V}$$
 (24)

where Δt_c is the increment within the time segment normalized to an hour. For a $15\,\mathrm{min}$ segment, $\Delta t_c=0.25$. The constrain on z^i is expressed as

$$\bar{z}^i \le z^i \le 1. \tag{25}$$

Hence, the optimization problem is composed of cost function (15, (19 and 20) and constrains (21, (23 and 25) and is given as

$$\min_{\mathbf{P_c}} \quad \mathcal{J}_{el} + \mathcal{J}_{ca} + \mathcal{J}_{cy}
\text{s.t.} \quad \sum_{i=1}^{N} {}_{j}^{i} P_{c} \leq \hat{P}_{G}, \ \forall \ j \in \mathbb{T}
\bar{z}^{i} \leq z^{i} \leq 1, \ \forall \ i \in \mathbb{V}
\mathbf{P_c} \in \{\mathbb{P}_{c}\}^{n}$$
(26)

C. Optimization Algorithm

The optimization problem expressed in (26) is simplified by making an a priori assumption that the charging profile with minimum cost must be continuous. The statement is true in practice as pausing and re-staring a charging event requires additional energy and time which has an extra cost (compared to continuous charging). This implies that the rest period for the vehicle $(P_c = 0)$ must be at the beginning or end of the charging window. Hence, the length of charging window n^i for vehicle i can be split into

$$n^i = n_{r1}^i + n_c^i + n_{r2}^i,$$

where n_{r1}^i and n_{r2}^i are the number of time segments that has no charging at the beginning and end of the charging window, respectively. n_c^i is the remaining number of segments where charging can take place.

This definition helps split the optimization problem into two parts: charging and resting. The charging part can be solved separately by only evaluating cost functions and constrains which are affected by charging alone. The prime requisite during the charging process is for charge power $P_c>0$. Amongst the cost functions only (13 and 18) have sole dependency on P_c while cost function for calendar ageing (17) also contributes during rest. A vector $\tilde{\mathbf{P}}_{\mathbf{c}}$ can be defined containing the non-zero elements from $\mathbf{P}_{\mathbf{c}}$. The length of this vector is defined as

$$\check{n} = \sum_{i=1}^{N} n_c^i$$

Hence, the optimization problem for charging phase is formulated as

$$\min_{\check{\mathbf{P}}_{\mathbf{c}}} \quad \mathcal{J}_{el} + \mathcal{J}_{cy}$$
s.t.
$$\sum_{i=1}^{N} {}_{j}^{i} P_{c} \leq \hat{P}_{G}, \ \forall \ j \in \mathbb{T}$$

$$\bar{z}^{i} \leq z^{i} \leq 1, \ \forall \ i \in \mathbb{V}$$

$$\check{\mathbf{P}}_{\mathbf{c}} \in \{[\underline{P}_{c}, \bar{P}_{c}]\}^{\check{n}}$$
(27)

The resting part can be solved as a global optimization problem that minimized the cost function of (26). A new variable $\mathbf{n_r} = \{n_{r1}^1, n_{r1}^2, \dots, n_{r1}^N, n_{r2}^1, n_{r2}^2, \dots, n_{r2}^N\}$ is defined which characterizes the rest period at the beginning and end of the charging window. This global optimization problem is formulated as

$$\min_{\mathbf{n_r}} \quad (27) + \mathcal{J}_{ca}
\text{s.t.} \quad n_{r1}^i + n_{r2}^i < n^i, \ \forall \ i \in \mathbb{V}
0 \le n_{r1}^i, n_{r2}^i \le n^i, \ \forall \ i \in \mathbb{V}.$$
(28)

The original optimization problem (26) is non-linear making it computationally expensive. However, the new global optimization problem (28) has only integer variables and hence, can be efficiently solved with a Non-linear Integer Programming Problem (NIPP). Likewise, the embedded optimizaton problem (27) is linear in $\hat{\mathbf{P}}_{\mathbf{c}}$ and can be solved as a Linear Programming Problem (LPP). This makes the new problem formulation computationally more efficient compared to the

original. The NIPP is solved using Genetic Algorithm (GA) and LPP using Linear Programming (LP).

IV. RESULTS AND DISCUSSION

In this section, the optimization algorithm is applied to a real-world case study and compared against a greedy optimization benchmark. The objective of greedy optimization is to charge the vehicle as early as possible within the boundary condition of the problem.

A. Case Study

A case study is taken for a fleet of EU N1 category BEVs operating within the Netherlands. Table I gives the list of parameters used in the optimization. Maximum grid capacity is taken from a standard electricity connection available for commercial application within the Netherlands. For charger model, maximum and minimum power is taken from the specification of the on-board charger of the vehicle. The slope and intercept for the charger model are computed from a reference charger efficiency map as shown in Section II-D. The parameters for ageing model are identified from in-house accelerated ageing test for the battery pack. The price and charge capacity is taken from the specification of the battery.

TABLE I: Model parameters for the optimization problem.

Parameter	Symbol	Value	Unit							
Grid										
Maximum Power	$ \bar{P}_G $	100	kW							
Charger Model										
Maximum Power	$ \bar{P}_c $	11	kW							
Minimum Power	$ P_c $	0.5	kW							
Slope	$ m_c $	1.052	-							
Intercept	$ b_c$	0.3951	-							
Ageing Model										
Parameter Calendar Ageing	$ b_4 $	3.58E-05	-							
	$ a_1 $	7.12E+05	-							
Parameter Cyclic Ageing	a_3	2.16E+03	-							
Battery Model										
Price	$\mid \mathcal{E}_{bat}$	1700	€							
Capacity	$ $ \bar{C}_B	20.16	kWh							

The optimization scheme is first applied to a single vehicle and then extended to fleet of multiple vehicles. In terms of scheduling, two test scenarios are considered:

- Opportunity Charging: The vehicles come to the hub in the middle of the day and have a small window of opportunity for charging;
- Overnight Charging: The vehicles are parked overnight at the charging hub and have until morning to charge before their shift begins.

B. Single vehicle Optimization

Fig. 8 shows the results from the optimization scheme for a single vehicle during an opportunity charging event. The vehicle has a small window of a few hours in the middle of the day (between 12:15 to 15:45) to charge from 47% to 88%. It is seen that the greedy optimization schedules the vehicle to charge at maximum charging power of $11\,\mathrm{kW}$ at the beginning of the charge window. The optimal charging scheme also charges the vehicle with maximum charging power but schedules the charging as late as possible.

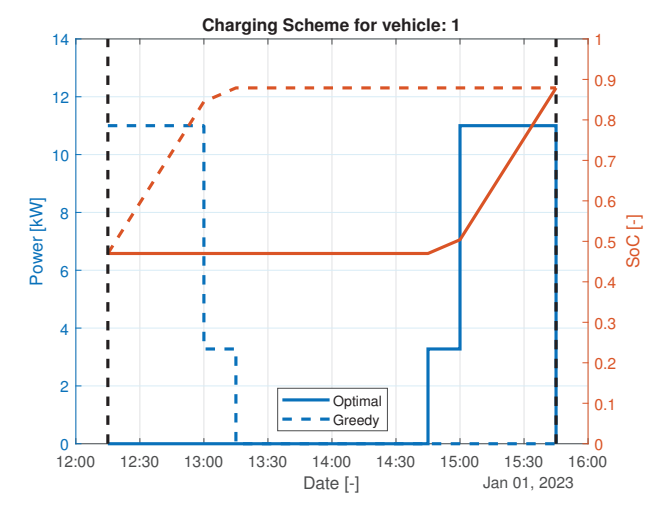


Fig. 8: Optimization result for a single vehicle during Opportunity Charging.

Fig. 9 gives the cost of charging for the optimal and greedy schemes shown in Fig. 8. For both methods, the dominating cost is electricity from the grid. This cost is same between the optimal and benchmark scheme as the total power drawn from the grid is same for both cases. The cost due to cyclic ageing is also same as charge power applied to the vehicle during both cases mirror each other. The difference in cost comes from calendar ageing, where early charging results in 1.5 times higher cost than late charging. This is because the battery undergoes faster deterioration from calendar ageing at higher SoC. This is also the reason why charging as late as possible is the optimal solution because the particular parameters selected for ageing (and their resulting costs) gives more relevance to calendar ageing than to cyclic ageing. Notice that in case of a parameter combination with a stronger cyclic ageing effect, the charging scheme is likely to be distributed during the day.

Fig. 10 shows the results from optimization scheme for a single vehicle during an overnight charging session. Here, the vehicle has a higher charging requirement from 18% to 89%. The greedy algorithm shows similar results as opportunity charging but the optimal charging scheme completes by 07:00 i.e., one hour before the end of charging time window. This is because the cost of electricity increases in the morning from 07:00 onwards and the algorithm does a trade off to minimize grid cost over calender ageing.

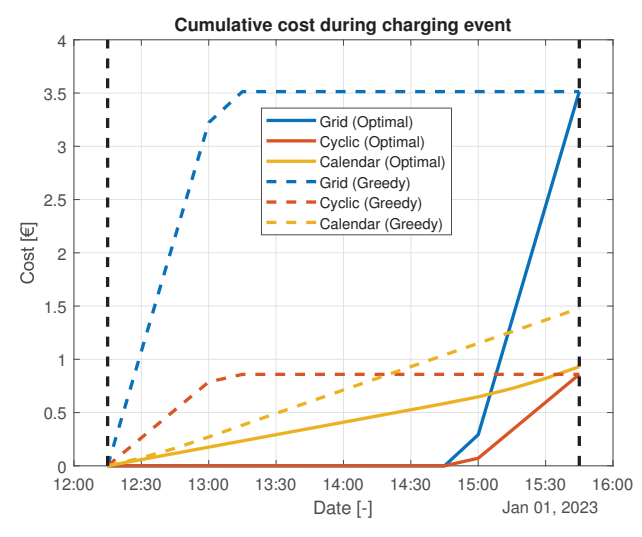


Fig. 9: Cost of charging for a single vehicle during Opportunity Charging.

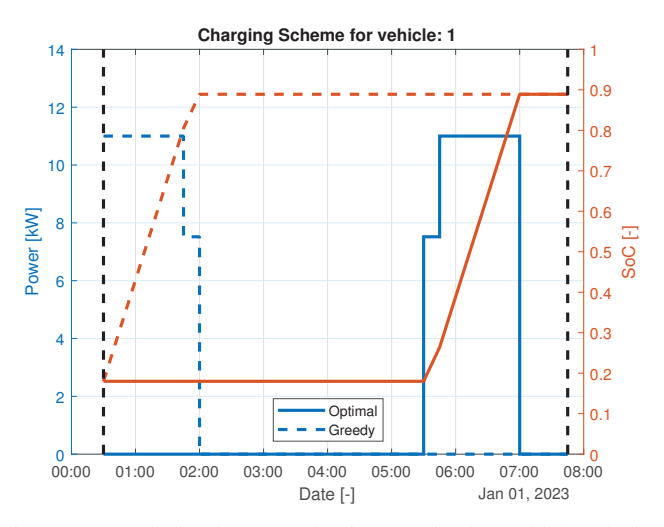


Fig. 10: Optimization result for a single vehicle during Overnight Charging.

Fig. 11 shows the costs from the charging schemes of Fig. 10. In this case, the grid and cyclic ageing costs are the same while the calendar ageing is almost 3 times larger. It is seen that the optimized scheme has a stronger impact on charging cost when the charge window is longer.

C. Fleet-level Optimization

Fig. 12 shows the optimal charging scheme for a fleet of 20 vehicles during overnight charging. Similar to single vehicle optimization, here each vehicle individually tries to charge as late as possible while not violating any boundary conditions. The total power drawn from the grid slowly increases to the maximum of $100\,\mathrm{kW}$ and drops rapidly at 07:00 when the electricity prices increase.

The impact of charge scheduling algorithm also becomes significant for large fleet of vehicles. This is seen in Fig. 13 where the cost of greedy optimization has a massive increase

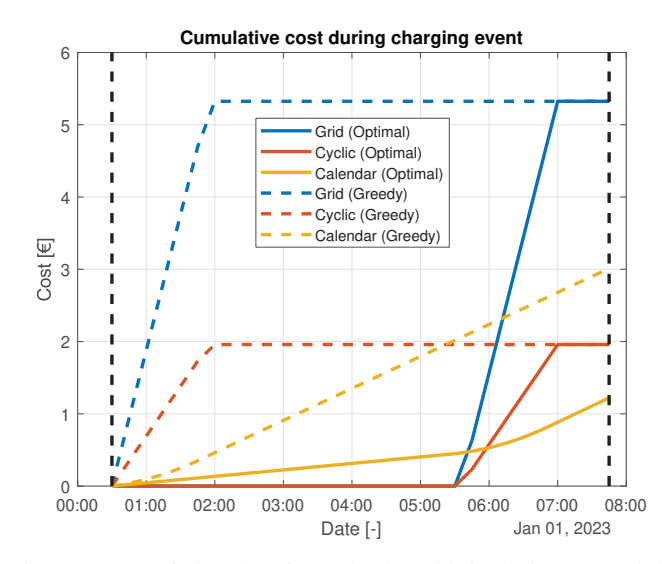


Fig. 11: Cost of charging for a single vehicle during Overnight Charging.

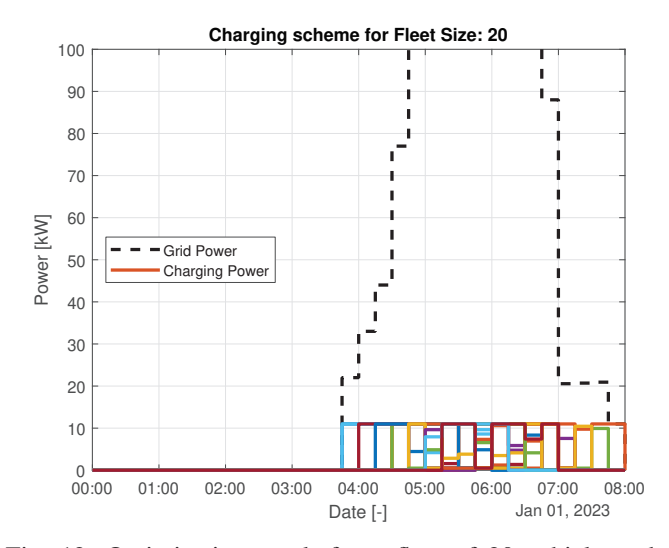


Fig. 12: Optimization result for a fleet of 20 vehicle under Overnight Charging.

with the increase in fleet size. It is seen that optimal solution saves \le 216.12 for a fleet of 200 vehicles compared to greedy-charging algorithm. This gives a total cost saving of 13% or \le 1.08 per vehicle per charging session.

Fig. 14 shows the increase in simulation time with the increase in fleet size. It is seen that even for a large fleet of vehicle the algorithm is relatively fast. For the test case in this work, it takes less than 160 sec for a fleet of 200 vehicles. This makes the algorithm suitable for real-time implementation.

V. CONCLUSIONS

In this study, an optimal charge scheduling algorithm was developed for a fleet of BEVs to minimize fleet operation costs. To make the algorithm feasible for real-time implementation, several simplifications were proposed, including dividing the optimization algorithm into a Non-Linear Integer

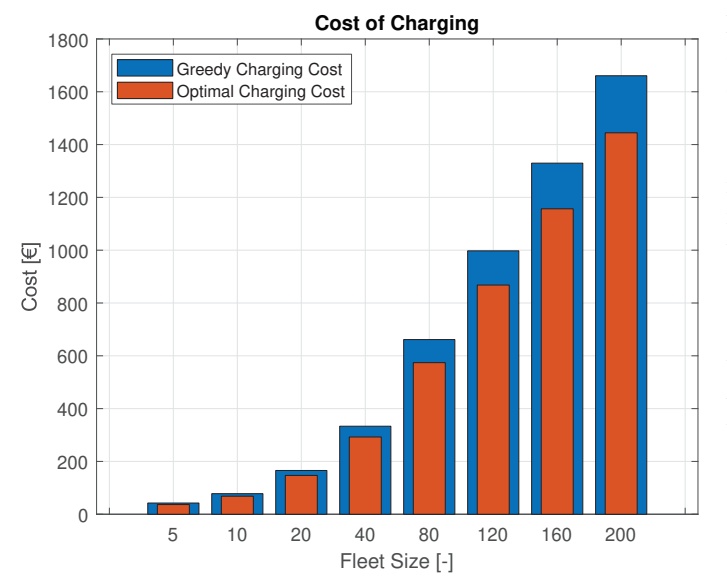


Fig. 13: Cost of charging for the fleet scheduling algorithm.

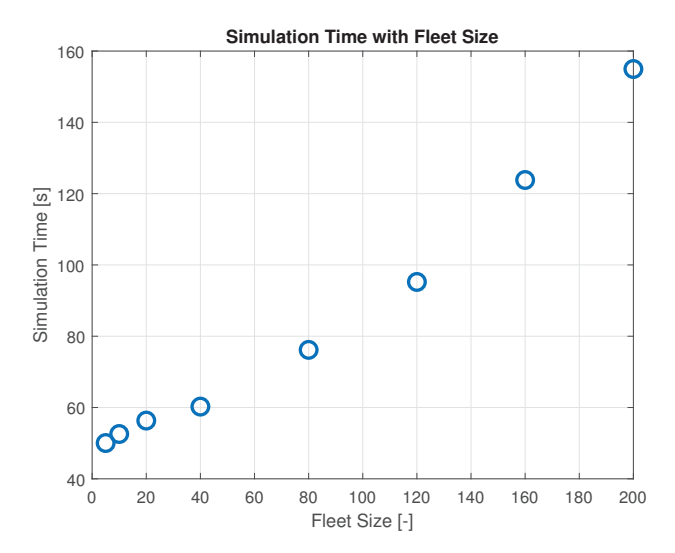


Fig. 14: Simulation time for the fleet charging scheduling algorithm.

Programming Problem and a Linear Programming Problem, and simplifying the battery ageing model to consider only conditions directly affected by the charging strategy.

Simulation results showed that the optimal strategy was to charge as late as possible, as calendar ageing had the most significant impact on cost. Compared to a greedy charging strategy, the optimal solution saves 13% on total cost of operation, with an execution time of less than 160 s, making it feasible for real-time implementation.

Future work will extend this method to include scenarios with fewer chargers than vehicles, which is likely as more BEVs are added to commercial fleets while grid capacity remains limited. Additionally, the battery dynamics will be extended to include non-linear charging behaviour at high SoC caused by constant voltage phase of the charging procedure.

Lastly, the algorithm will be extended to generate a suboptimal solution in case of infeasibility for the required charging conditions.

In conclusion, the proposed algorithm provides a promising solution for managing the charging of a fleet of BEVs to minimize operation costs. With further development and extension, it has the potential to play a significant role in the transition to sustainable transportation.

ACKNOWLEDGMENT

This research has received funding from the European Union's Horizon 2020 research and innovation programme under grant agreement No 101006943, under the title of URBANIZED (https://urbanized.eu/).

REFERENCES

- [1] V. Masson-Delmotte et al., "Summary for Policymakers. In: Climate Change 2021: The Physical Science Basis. Contribution of Working Group I to the Sixth Assessment Report of the Intergovernmental Panel on Climate Change," IPCC, Tech. Rep., 2021.

 Z. Zhongming et al., "Companion to the Inventory of Support Measures
- for Fossil Fuels 2021," OECD, Tech. Rep., 2021.
- W. J. Smith, "Can EV (electric vehicles) address Ireland's CO2 emissions from transport?" Energy, vol. 35, no. 12, pp. 4514-4521, 2010.
- N. times, "Dutch power grid overloaded in more places; connections possible)," https://nltimes.nl/2022/08/04/ No new dutch-power-grid-overloaded-places-new-connections-possible, accessed: 2023-03-08.
- "Beschikbaarheid capaciteit [5] Liander. per gebied (Available region)," capacity https://www.liander.nl/transportschaarste/ per beschikbaarheid-capaciteit, accessed: 2022-04-27.
- [6] J. A. P. Lopes, F. J. Soares, and P. M. R. Almeida, "Integration of electric vehicles in the electric power system," Proceedings of the IEEE, vol. 99, no. 1, pp. 168-183, 2010.
- [7] B. Xu et al., "Modeling of lithium-ion battery degradation for cell life assessment," IEEE Trans. on Smart Grid, vol. 9, no. 2, pp. 1131-1140,
- [8] R. Carli and M. Dotoli, "A distributed control algorithm for optimal charging of electric vehicle fleets with congestion management," IFAC-PapersOnLine, vol. 51, no. 9, pp. 373-378, 2018.
- [9] M. Rogge et al., "Electric bus fleet size and mix problem with optimization of charging infrastructure," Applied Energy, vol. 211, pp. 282-295,
- A. Houbbadi et al., "Multi-objective optimisation of the management of electric bus fleet charging," in 2017 IEEE Vehicle Power and Propulsion Conference (VPPC). IEEE, 2017, pp. 1-6.
- "Optimal scheduling to manage an electric bus fleet overnight charging," Energies, vol. 12, no. 14, p. 2727, 2019.
- [12] L. Zhang, S. Wang, and X. Qu, "Optimal electric bus fleet scheduling considering battery degradation and non-linear charging profile." Transportation Research Part E: Logistics and Transportation Review, vol. 154, p. 102445, 2021.
- [13] D. Geerts et al., "Optimal charging of electric vehicle fleets: Minimizing battery degradation and grid congestion using battery storage systems," in 2022 Second International Conference on Sustainable Mobility Applications, Renewables and Technology (SMART). IEEE, 2022, pp.
- [14] C. Song et al., "Joint estimation of soc and soh for single-flow zincnickel batteries," Energies, vol. 15, no. 13, p. 4781, 2022.
- [15] Y. Abdul-Quadir et al., "Heat generation in high power prismatic li-ion battery cell with limnnicoo2 cathode material," International Journal of Energy Research, vol. 38, no. 11, pp. 1424-1437, 2014.
- J. Schmalstieg et al., "From accelerated aging tests to a lifetime prediction model: Analyzing lithium-ion batteries," in 2013 World electric vehicle symposium and exhibition (EVS27). IEEE, 2013, pp. 1–12.